THREE-DIMENSIONAL THERMAL HYDRAULIC ANALYSIS OF A TRANSPORTABLE FLUORIDE-SALT-COOLED HIGH-TEMPERATURE REACTOR

Chenglong Wang
Department of Nuclear Science and Technology, Xi'an Jiaotong University
MIT Nuclear Reactor Laboratory, Massachusetts Institute of Technology
138 Albany Street, Cambridge, MA, 02139, U.S.
chlwang@mit.edu

Kaichao Sun, Lin-wen Hu*
MIT Nuclear Reactor Laboratory, Massachusetts Institute of Technology
138 Albany Street, Cambridge, MA, 02139, U.S.
kaichao@mit.edu ; lwhu@mit.edu

Suizheng Qiu, Dalin Zhang
Department of Nuclear Science and Technology
Xi'an Jiaotong University
28 Xianning West Rd., Xi'an, Shaanxi, 710049, China
szqiu@mail.xjtu.edu.cn; dlzhang@mail.xjtu.edu.cn

ABSTRACT

A 20MWth Transportable small reactor with Fluoride-salt-cooled High-temperature Reactor (TFHR) technology is proposed by Massachusetts Institute of Technology for off-grid applications. In this paper, the preliminary thermal-hydraulic analyses and improvements based on $1/12^{th}$ TFHR full core model have been performed using 3-D computational fluid dynamics (CFD). Three practical considerations that may challenge the TFHR limiting safety and system settings (LSSS) are evaluated in conservative manners. These include 1) helium gap between fuel compact and graphite block, 2) thermal property degradations of graphite matrix due to neutron irradiation, and 3) actual power profile with non-uniform distribution. The conservative approaches lead to insufficient margin between the normal operating conditions and the safety limits. Furthermore, additional measures, including bypass cooling and flow re-distribution, are made to improve the thermal-hydraulic safety of the TFHR. Overall, a more flattened temperature distribution with the lower peaking temperature of fuel and coolant across the TFHR core has been achieved. No thermal-hydraulics limit is exceeded for the operating condition of 20% over-power, i.e., with 24 MWth.

KEYWORDS
Transportable small reactor; FHR; CFD; Thermal-hydraulics

1. INTRODUCTION

There is a potential small reactor market for Antarctic bases, remote mining sites, container ships, military bases and other off-grid applications. In many cases, it is desirable that the reactor has a compact design

and can be easily transported by a truck, or a train or an airplane. The cost of electricity and heat from conventional sources for remote locations is often very high and therefore a compact nuclear reactor design is an attractive option in spite of higher capital cost per kW than a conventional nuclear reactor. The FHR would be sized for the average demand resulting in a much smaller, more transportable, and more economic reactor compared to other nuclear energy technologies [1]. Smaller reactor sizes often allow for major simplification of systems, especially safety systems. As a result, a more compact core configuration can be achieved with the FHR technology. Within the framework of FHR project, a conceptual design of 20 MWth compact Transportable FHR (TFHR) with 18-month, or 550 effective full power days (EFPDs), one-through fuel cycle is on-going at MIT [2, 3]. This paper aims to evaluate the system operation safety and provide a licensing basis, emphasis being placed on the thermal-hydraulic features of the TFHR at the steady-state.

In the prismatic nuclear reactors, the complex geometry of fuel blocks brings certain challenges for accurate prediction of the fuel temperature. Hence, many researchers adopt simplified computational models for the analyses and designs of prismatic reactors. These models are the equivalent cylinder model and the unit cell model. The equivalent cylinder model, transformed from unit cell model by preserving the volume of each part, has been widely adopted in the thermal-fluid analyses of prismatic fuel by hand calculation or system analysis code [4, 5]. More accurate predictions have been conducted by solving a multi-dimensional heat conduction based on unit cell model that consists of two equivalent fuel rods and one coolant channel [6, 7] (see a unit cell in Fig.1). The unit cell model can be used to thermal-hydraulics analyses of some local area of prismatic core based on reasonable assumptions. These two simplified approaches are very helpful to understand basic aspects of heat transfer rapidly due to its largely reduced computational efforts, especially when applied to transient behavior study. However, they are only acceptable for a heat transfer unit of a full prismatic fuel block. They cannot consider the mutual heat transfer of different unit cells and the bypass flow between fuel blocks, which may practically affect the fuel temperature.

During the recent decades, owing to the remarkable progress in computational fluid dynamics (CFD) technology, as well as the performance of workstation, using 3-D CFD codes becomes more popular in thermal-hydraulics analyses of prismatic core nuclear reactors. Cheng et al. use the commercial software CD-adapco STAR CCM+ to study the effects of asymmetric power generation on thermal-hydraulics characteristics of FHTR [7]. They modeled a unit cell of TFHR in detail and assumed four types of power distributions. Tak et al. numerically analyzed a heat transfer with the $1/12^{th}$ prismatic fuel block of a VHTR using a commercial CFD code, ANSYS CFX [8]. The effects of bypass gap flow and the radial power distribution are investigated in this study. It has been found the bypass flow has a major impact to the VHTR thermal-hydraulics. Furthermore, Travis et al. numerically investigated $1/6^{th}$ core of VHTR with 3-D thermal conduction in fuel compact and graphite reflector coupled to 1-D helium flow model in order to reduce computation time and memory requirements [9]. They considered helium intestinal bypass flow in detail and also applied cosine and uniform axial power profiles in their model. It has been reported the accurate prediction of fuel temperature is largely dependent on the selection of helium heat transfer correlations.

There are also many other CFD efforts and publications corresponding to the prismatic reactor core, but most of them adopt helium as coolant and focus on the flow and heat transfer within fuel assembly not for full core level. More importantly, little work has been done to the effect of some practical considerations, such as gas clearance between fuel compact and graphite matrix, graphite thermo-physical properties degradation, and power deformation, which have considerable challenges to the TFHR LSSS limits. In the present paper, the above mentioned three considerations have been studied in conservative manners. The thermal hydraulic design features of $1/12^{th}$ prismatic TFHR core have been numerically evaluated from the viewpoint of reactor safety. The detailed temperature distribution and the heat transfer

coefficient have been obtained throughout the core. Two measures have been adopted to flatten the temperature distribution and lower the peak fuel temperature and coolant temperature.

2. TFHR DESIGN AT MIT

The concept of advanced TFHR is first proposed at MIT to meet potential government missions for ships and remote sites in 2013 [10]. Thereafter, Sun and Hu embody the prismatic core TFHR from the perspective of neutronics and have conducted the fuel cycle optimization using MCODE [2]. The primary coolant adopts a binary molten salt system of the 66.7% ^{7}LiF-33.3% BeF_2 (FLiBe) that is used successfully as a matrix salt for the MSRE fuel salt and performed excellently in those functions for the life of the experiments [11]. In addition, similar to the HTRs and VHTRs, TFHR adopts TRISO fuel particles, which are embedded randomly in a cylindrical carbonaceous matrix to form a fuel compact with packing fraction (PF) of 0.35. Burnable poison particles (BPPs) made of B_4C, which have similar layout as TRISO fuel particles but with poison materials as kernel, are adopted as key measure for minimizing the reactivity swing induced by fuel depletion and also prolonging the fuel cycle. They are randomly distributed in the fuel compacts. Stacks of fuel compacts are then inserted into hexagonal graphite matrix to construct a fuel blocks. Due to fabrication issue of fuel compacts, a very small gap exists between the fuel compact and graphite matrix. Fig. 1 shows the geometry structure of TFHR's fuel block. Plots (a) is perspective of TRISO fuel particle, plots (b) is the horizontal schematic of fuel compact, and plots (c) is the view of prismatic fuel block.

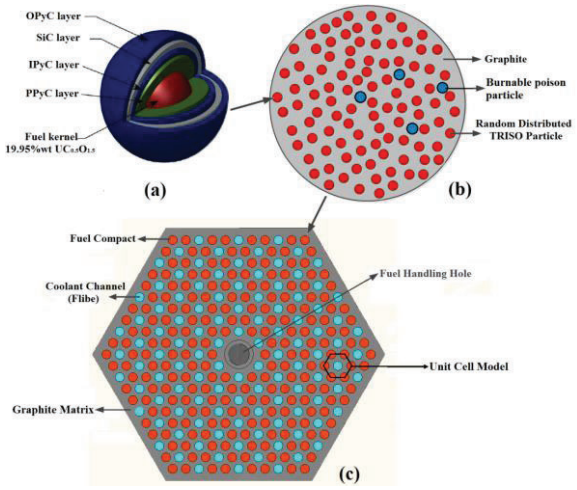

Figure 1. The schematic of TFHR's fuel block.

The top view and elevation view of the reactor core are shown in Fig. 2. The proposed 20 MWth TFHR is a hexagonal prism that mainly consists of four parts: central instrument channels (including central down-comer and control rods), active zone, replaceable graphite reflector (including safety rods) and permanent beryllium reflector. The active zone contains 18 fuel blocks, where the inner ring has 6 blocks and outer ring has 12 blocks (see Fig. 2(a)). At the central position of core, there are six control rods with independent control drive systems. There are also 12 safety rods distributing in the core periphery. Above and below the active zone, it has upper and lower graphite reflectors with coolant channels in order to enhance neutron economy and maintain flow hydro-dynamically developed (see fig. 2(b)). The outermost layer of core is the easily-transported and assembled beryllium reflector.

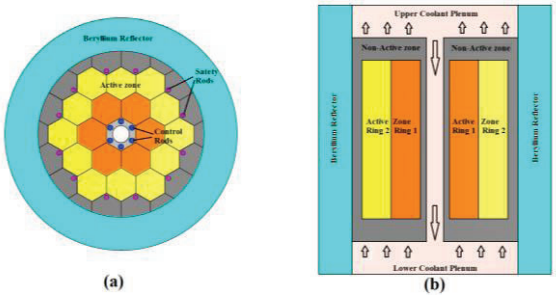

Figure 2. Horizontal and verical cross-section of TFHR.

3. NUMERICAL ANALYSIS

There is a geometrical symmetry for the prismatic layout. Accordingly, the 3-D thermal hydraulics analysis is carried out using a $1/12^{th}$ core sector (see Fig. 1). The $1/12^{th}$ core consists of 162 equivalent coolant channels (including 13 in half-channels) and 324 equivalent fuel rods (including 6 in half-channels). With use of appropriate of flibe, the Reynolds number (Re) is calculated to be 638 based on the assumed average flow rate of 0.043 kg/s per coolant channel. The flow in active zone is thus in laminar regime.

Different components of fuel blocks, outer graphite reflector and beryllium reflector, are included in the core model. STAR CCM+ could generate meshes for each component separately. They are jointed together thereafter. The meshing for the fuel block is the more important than that for comparing to the other parts. In this paper, the polyhedral and prism layer meshers are used to generate a layer mesh. The meshes along the flow direction are generated with extruder mesher. In order to keep a reasonable mesh number without consuming too much computational time, sensitivity study has been carried out by testing five cases (A, B, C, D and E) with different meshing schemes for a $1/6^{th}$ fuel block. Key thermal-hydraulic parameters, including outlet coolant bulk temperature T_b, average wall temperature $T_{w,avg}$ and the maximum fuel temperature $T_{fuel,max}$, are compared in Table I.

Table I. Mesh sensitivity study

Case	A(ref)	B	C	D	E
Mesh Number (million)	9.84	6.22	3.65	1.05	0.7
Base Size in Coolant(mm)	0.8	0.8	0.8	1.2	2.0
Base Size in Fuel & Graphite (mm)	1.0	3.0	5.0	8.0	10.0
Axial size (mm)	8.5	8.5	8.5	26.0	26.0
T_b (K)	972.8	972.7	972.2	972.1	969.6
T_b Relative Error, %	-	0.1%	0.6%	0.7%	3.2%
$T_{w,avg}$ (K)	1195.4	1195.0	1193.0	1192.3	1183.4
$T_{w,avg}$ Relative Error, %	-	0.4%	2.4%	3.1%	12%
$T_{fuel,max}$ (K)	1364.9	1364.4	1362.0	1361.3	1347.0
$T_{fuel,max}$ Relative Error,%	-	0.5%	2.9%	3.6%	17.9%
ΔP (Pa)	443.5	443.8	444.2	444.0	452.6

As seen in Table I, the mesh number decreases from Case A (9.84 million) to Case E (0.7 million). The compared parameters remain largely unchanged except for Case E, which has a notable discrepancy to

other cases. It is thus clear that Case D is the optimal choice for full core simulation with consideration of both computation time and accuracy. The detailed mesh scheme is shown in Fig. 3.

Reliable thermo-physical properties of flibe are of great importance. Ref [5] recommended flibe thermal properties on the basis of existing experimental data and fitting equations on fluoride salts. The thermal properties of other components, such as graphite, fuel compact, beryllium reflector and helium are adopted from the design report of very high and high temperature gas cooled reactors (VHTRs or HTGRs) [6].

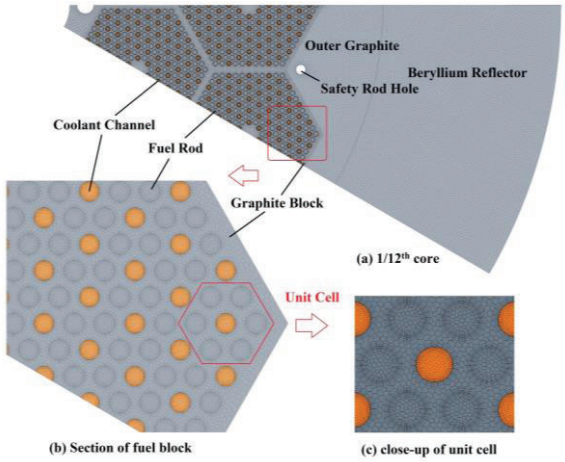

Figure 3. Mesh details of 1/12th TFHR core (Case D).

Once the numerical mesh grid is generated and employed, performing the thermal-hydraulics analyses is relatively straightforward. The parametric input consists of inlet temperature, mass flow rate of FLiBe in each coolant channel and fission power distribution. The inlet temperature is fixed at 873.15 K with total mass flow rate of 6.98 kg/s. The outlet is set to be a pressure outlet with a relative pressure of zero Pa for the purpose of fast convergence. The heat loss during the reactor operation is neglected. Therefore, the boundaries outside the TFHR core are set to be adiabatic no-slip wall or symmetry. The average volumetric power density in the fuel compact is 31.25 MW/m^3 for the base case.

Since there is no licensing experience for such a transportable small reactor featured with multi-functions at remote site, the LSSS of the 20MWth FHTR, aiming to test fuel and material in realistic reactor environments, is adopted in this paper as thermal constraints for TFHR. The Nuclear Regulatory Commission (NRC) defines safety limits (SL) and limiting safety system settings (LSSS) for licensing. Generally, the LSSS will ensure that automatic protective action will correct the abnormal situation before a safety limits is exceeded [12]. As a result, the LSSS defines the operating region of the nuclear reactor. The thermal boundary provide safe margin over the designed operating region to ensure the integrity of the structural material and fuel. Four thermal limits are derived from the materials used in FHTR [5], as tabulated in table II.

Table II. LSSS criteria of FHTR

Constraints	**Value**	**Material**
Minimum Inlet temperature, T_{in}	783 K	FLiBe
Maximum outlet bulk temperature, T_{out}	993 K	Hastelloy N
Maximum coolant temperature, $T_{c,M}$	1473 K	FLiBe

Maximum fuel temperature, $T_{f,M}$	1573 K	TRISO

4. RESULTS AND DISCUSSION

4.1. Thermal-hydraulic Analysis of 1/12th TFHR Core

Our previous study [13] has validated the CFD models of FLiBe flow and heat transfer. In this section, the thermal-hydraulic analysis is performed in terms of calculating the temperature distributions of the 1/12th TFHR core. The effects of gas clearance between fuel compact and graphite matrix, graphite thermo-physical properties degradation and power deformation that may challenge the TFHR LSSS are then evaluated in a conservative manner to find the deficiency of the current design.

4.1.1. Results for the base case

The results of the thermal-hydraulics analyses for the TFHR base case are presented in Fig. 4. With uniform power profile, the temperature distribution results at the outlet section are presented. Overall, the temperature distribution is largely flat throughout the entire active zone. Hot spots are found at the joint corners of the fuel blocks, where there are less coolant channels in these regions. The temperature of the corresponding fuel rods peaks at 1358.6 K, which is about 160 K higher than volumetric-averaged fuel temperature. The hottest coolant channel is located in the same region, close to fuel rods with the highest temperature. As mentioned earlier, due to high viscosity and low thermal conductivity of FLiBe, the flow condition in coolant channel is in the laminar regime, so that a relatively cold region (accounts for 8% of total area) exists in the coolant channel (see Fig. 4). The highest temperature of coolant reaches 1320.5 K adjacent to the heated wall.

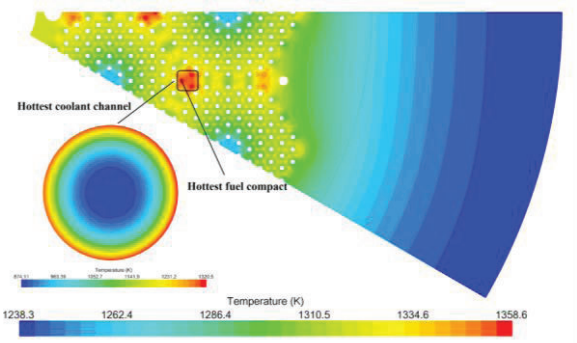

Figure 4. Outlet temperature distribution of 1/12th TFHR core for base case.

4.1.2. Effects of gas clearance, graphite properties degradation and power deformation

1) Gas clearance between fuel compact and graphite matrix

There is typically a small gas gap exists between the fuel compact and graphite matrix. On the one hand, it is due to certain limitations during fuel block assembling. On the other hand, the gas volume could help retain the radioactive substances released from fuel compacts. The gap width of Liquid-Salt-cooled Very High-Temperature Reactor (LS-VHTR) designed by ORNL (i.e. 0.127 mm) is adopted in this study, since the LS-VHTR has similar fuel block design to the current TFHR. In reality, the thermo-physical properties in clearance, which vary as the fuel reacts and daughter constituents fill the space, cannot be

easily concluded. It thus has great difficulties in direct simulating this region at full core level. For the sake of simplicity, the clearance assumed with full of helium is treated as an empirical contact thermal resistance in 3-D simulation, with its thickness added to the fuel. The radiation and natural convection are neglected due to small temperature drop across fuel-graphite interface based on the following results.

2) Graphite thermo-physical properties degradation due to neutron irradiation

It is a well-known issue that the neutron irradiation could remarkably deteriorate the thermo-physical properties of graphite. The corresponding thermal-hydraulic effect is thus carefully evaluated in the present paper. According to the study of Maruyama and Harayama [14], the variation of the graphite thermal conductivity becomes very small at high temperature (above 1350 K), but there still remains a large thermal conductivity difference between irradiated and unirradiated graphite. This difference does not increase after the fast neutron fluence exceeds 3×10^{25} n/m^2. For the TFHR, the calculated peak fast neutron fluence is 3.2×10^{25} n/m^2 corresponding to the end-of-life fuel cycle state. Thus, the thermal conductivity ratio of irradiated to unirradiated graphite is assumed as a constant. The ratio of 0.67 is adopted for conservative considerations [4].

3) Power deformation based on 3-D neutronic outputs

Many thermal-hydraulic studies for the prismatic reactors are based on uniform power density, or fitted cosine power correlation. These may result in a more flattened the temperature distribution and a lower the maximum temperatures of fuel and coolant (see Fig. 4). It is thus not a conservative approach for nuclear reactor thermo-condition analyses. In this paper, a full core level power profile based on 3-D neutronic outputs is coupled to the 3-D CFD model, in order to predict the best-estimate temperature distribution. The calculated power profile at the Beginning Of Life (BOL) is adopted for the non-uniform case, since the highest power local peaking factor occurs, when the control rods are inserted at their lowest positions. This, in turn, might lead to a significant distortion of the temperature distribution. Fig. 5 shows the distribution of power peaking factors in the TFHR. The maximum power factor occurs at outermost of the active core, peaking at 2.18. It is followed by a high power factor region across the interface between active core and outer graphite reflector. The minimum power factor, as low as 0.24, occurs at top central side of active core due to the nearby inserted control rods.

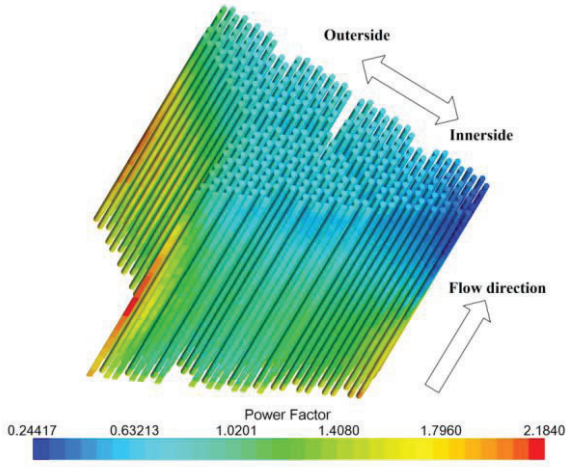

Figure 5. Power factor distribution of TFHR core.

For convenience, the case with consideration of all above three practical concerns is named as the "limiting case". Fig. 6 presents the outlet temperature distribution of 1/12th TFHR core for the limiting case. It can be seen that a significant temperature change occurs across the entire outlet compared to the base case (as shown in Fig. 4). The hot spots shift towards core periphery due to the higher power peaking factors in this region (f_{peak}=1.6~2.2, see Fig. 8), leading to a wider temperature range, from 1147 K to 1479 K. In addition, the higher temperature in the core periphery leads to higher coolant and reflector temperature (1400 K and 1370 K, respectively). Fig. 7 compares the temperature distribution between the base case and the limiting case at the P1 symmetry plane (defined in Fig. 6). Compared to the base case, the peak temperature relocates from the outlet to the upper middle part of the core due to the deformed power profile (see Fig. 5., The peak temperature in the limiting case is notably higher by ~205 K. Nevertheless, this is still lower than the maximum allowed TRISO particle operating temperature of 1573 K. Furthermore, no sub-cooled boiling of the coolant is anticipated to occur, since no liquid-wall interface temperature is found to reach the flibe boiling limit of 1473 K.

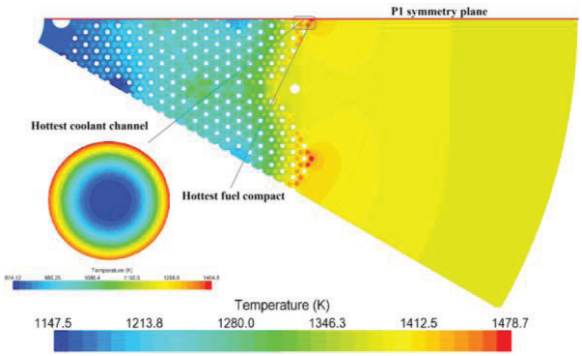

Figure 6. Outlet temperature distribution of 1/12th TFHR core for limiting case.

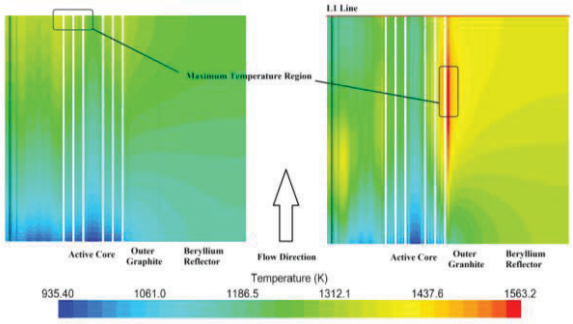

Figure 7. Temperature distributions at P1 symmetry plane for base case (left) and limiting case (right).

The details about separating the individual effects of three practical considerations along the L1 line are illustrated in Fig. 8. Compared to the effects of helium clearance and graphite property degradation, the non-uniform power density has more remarkable influence on thermal-hydraulic characteristics of the TFHR, leading to a larger temperature fluctuation throughout the entire core. The existence of helium clearance just raises the fuel compact temperature by 30 K in average. For effect of graphite thermal properties degradation due to neutron irradiation, the temperature in the active zone is generally increased by ~ 10 K. The insignificant effect can be explained by two reasons. The first is that higher thermal conductivity of graphite (40 W/m-K) after intensive neutronic irradiation can be found in high temperature condition [4]. The second is that the heat transfer length (about 8 mm) between fuel compacts

and coolant channels is short. The local enlarged view in Fig. 8 shows that for high temperature region, the temperature rise due to the deformed power profile accounts for 55-65% in total fuel temperature increase, while the effects of helium clearance and graphite properties degradation contribute only about 20% and 10 %. It is also noteworthy that all the practical considerations have little effect on the FLiBe temperature at the central part of coolant channel; whereas the temperature adjacent to the wall is affected significantly.

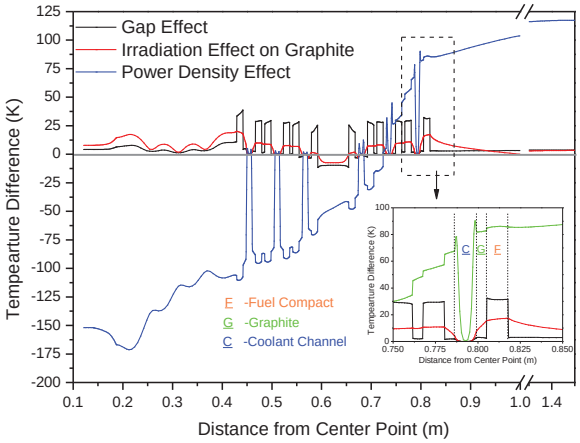

Figure 8. Effects of gas clearance, graphite properties degradation and power deformation on temperature distribution along the L1 line.

According to the FHTR LSSS Criteria, the key thermal-hydraulic parameters comparison of the base and limiting cases are listed in Table III. The temperature margins for the maximum fuel and coolant temperatures are reduced from 214.4 K to 9.8 K and 143.3 K to 16.3 K, respectively. The TFHR design may not be able to meet all the safety requirements; if the 20% overpower condition (LSSS) is considered. At the next step, some measures will be taken to lower the maximum fuel and coolant temperatures and flatten the temperature distribution throughout the core.

Table III. Key thermal-hydraulic parameters of different operating conditions

LSSS limits (K)	Maximum fuel temperature			Maximum coolant temperature		
	Calculated results	Thermal limit	Temperature margin	Calculated results	Thermal limit	Temperature margin
Base case	1358.6	1573	214.4	1329.7	1473	143.3
Limiting case	1563.2	1573	9.8	1456.7	1473	16.3

4.2. Improvements with Use of Thermal-hydraulic Measures

1) Bypass cooling at core periphery

It has been recognized that the bypass flow in the interstitial gaps between the prismatic fuel blocks in a VHTR core is inevitable. The gaps between fuel blocks are initially present because of the manufacturing tolerances, but their width varies with the fuel burn-up due to graphite swelling by neutron irradiation. According to the study of Boyce et al [9], the bypass flow could help in mitigating the hot spots at the

edge of fuel block. The bypass flow gaps are thus adopted to lower the maximum fuel temperature and coolant temperature for the TFHR, which has peak temperatures at the core periphery (see Fig. 6). The gap width of 5mm (VHTR design parameter) is employed. The coolant flow rate in the gap is set to 11% of total mass flow rate according to 3-D simulation results in Ref [9]. It should be noted that only the gaps adjacent to the core periphery are directly simulated. The gaps between fuel blocks are neglected in order to save computational resource. The former accounts for 42% of the total bypass flow. Fig. 9 shows the geometry and meshing details of the interstitial gap.

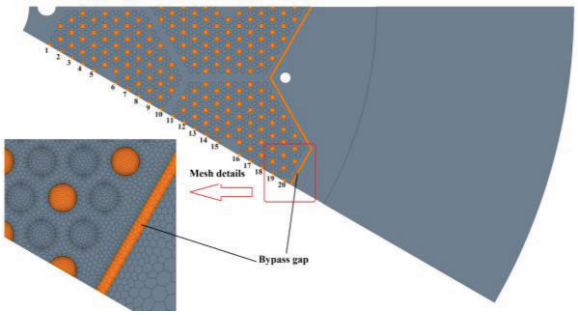

Figure 9. Geometry and meshing of bypass gap.

2) Coolant mass flow distribution

As presented in Fig. 2, the TFHR adopts the central coolant down-comer as the initial entrance to reactor core instead of conventional annular down-comer. This is mainly to make reactor core as small as possible, thus keeping TFHR more easily-transported. The improvement of mass flow distribution would flatten the temperature distribution throughout the active core and in turn lower the maximum temperatures. In this paper, three different heights of lower coolant plenum (0.3m, 0.4m and 0.5 m) are preliminary studied. There are other factors may affect the flow distribution of the TFHR, including the shape of plenum, orifice plates and other internal components. However, taking all these factors into consideration is not practical with use of CFD method and they are clearly beyond the scope of the present research. It should also be noted that the effect of heat transfer on flow distribution is neglect for simplicity. Fig. 10 presents the comparison of mass flow distribution among different heights of lower plenum. The numbers at x-axis represent the coolant channels defined in Fig. 9. It is found that the lower plenum of 0.3 m in height is more beneficial than those of 0.4 m and 0.5 m. The mass flow fluctuation is almost within 10% of nominal flow per channel, which shows good uniformity compared with other heights of lower plenum. More importantly, the mass flow in the edge of outer ring is a little higher than the nominal flow. This would be desirable for cooling the high temperature region at the core periphery (Fig. 6). Overall, the flow distribution from 0.3m height of lower plenum is adopted for the remaining study in this paper.

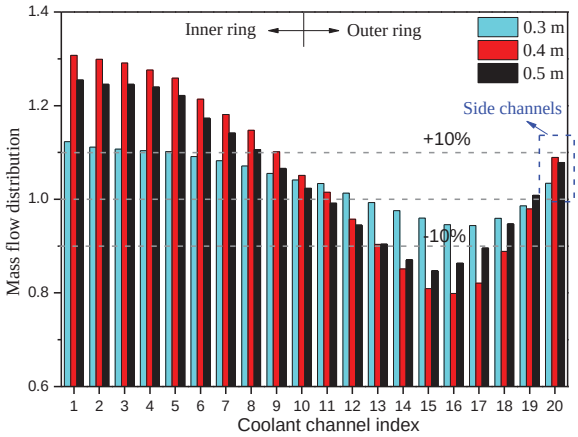

Figure 10. Mass flow distribution at different height of lower plenum.

With improvements of bypass cooling and flow distribution, the final temperature distributions of the 20 MWth TFHR core is presented in Fig. 11. Due to the existence of bypass flow at the core periphery (see Fig. 9) and higher allocated mass flow rate (see Fig. 10) in the same region, temperature peaks move towards the core center and the temperature distribution becomes more flattened, as compared with Fig. 6. The maximum temperatures of fuel compact and coolant are reduced from 1563.2 K and 1456.7 K to 1403.5 K and 1302.5 K, respectively. In addition, due to the low thermal conductivity of FLiBe and the laminar flow in bypass channel, little heat is transferred from active core to the outside reflectors. It leads to a much lower temperature in the outside reflectors. This, in turn, would improve the energy economic of TFHR and extend the operating lifetime of the permanent reflector.

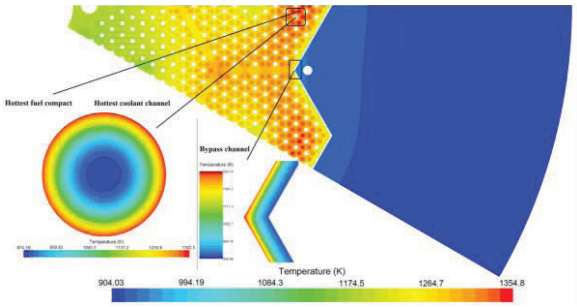

(a) Outlet temperature distribution

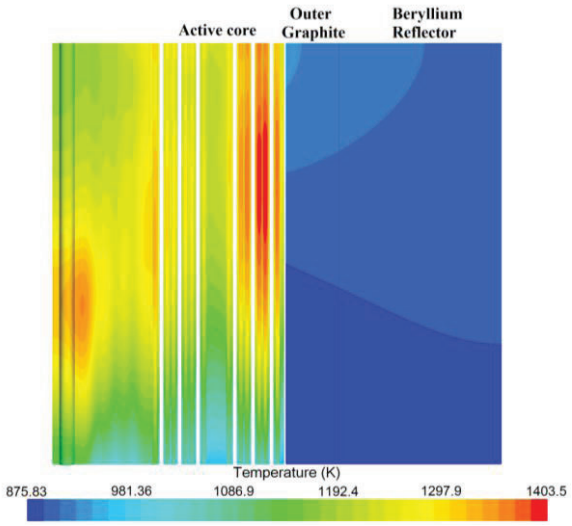

(b) Axial temperature distribuion at P1 symmetry plane

Fig. 11 Temperature distributions of 1/12th TFHR core after improvements

Fig. 12 shows more details on temperature improvents at the hottest channel. Due to the control rod insertion, the fuel compact and graphite temperatures peak at 0.85 m height of reactor core; whereas the coolant bulk temperature has a linear increase for obvious reasons. Compared with the limiting case, the volumetric-average temperatures for fuel and graphite decrease by 156 K and 127 K respectively. As a consequence, it leaves a larger temperature margin. Overall, the improvements of bypass cooling and mass flow distribution play a positive role for safety operation of the TFHR.

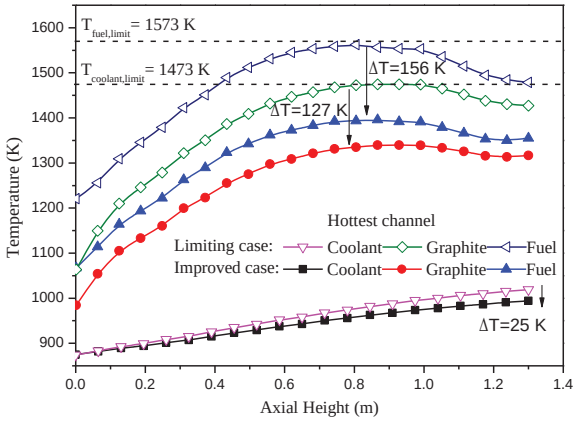

Fig. 12 Temperature comparison between unimproved and improved cases at hottest channel

In order to meet the conventional licensing requirements, the designed nuclear reactors should experience at most 20% over-power operation scenario [12] and all key thermal-hydraulic parameters should be within the LSSS limits. Table IV lists key thermal-hydraulic parameters of different operating conditions. It can be seen that there is still a relative large temperature margin for the fuel compact and FLiBe for 20% over-power condition. Overall, the current study shows the preliminary TFHR core design is practical and feasible from the thermal-hydraulic viewpoint.

Table IV. Key thermal-hydraulic parameters of different operating conditions

LSSS limits	Maximum fuel temperature (K)			Maximum coolant temperature (K)		
	Calculated results	Thermal limit	Temperature margin	Calculated results	Thermal limit	Temperature margin
Limiting case	1563.2	1573	9.8	1456.7	1473	16.3
Improved case	1422.7	1573	150.3	1315.6	1473	157.4
Over-power case (24MW)	1530.1	1573	42.9	1401.3	1473	71.7

5. CONCLUSIONS

Full core level 3-D thermal-hydraulic analyses of the Transportable Fluoride-salt-cooled High temperature Reactor (TFHR) have been investigated using CFD modeling. Coupled conduction and convection heat transfer is considered. The effects of three practical considerations, including 1) helium gap between fuel compact and graphite block, 2) thermo-physical properties degradations of graphite matrix due to neutron irradiation, and 3) actual power profile with non-uniform distribution, that may challenge the TFHR LSSS limits are evaluated in conservative manners. Finally, bypass cooling and flow distribution are adopted to improve the thermal-hydraulic behavior of the TFHR from the nuclear safety viewpoint. The major findings are summarized as follows:

1) For the base case with uniform power profile, hot spots occur at the joint corners of fuel blocks due to less coolant channels in the local region. While for the limiting case, hot spots shift from inner side to the core periphery, leading to much higher temperature peaks. This significantly reduces the temperature margin from 214 K (base case) to 10 K for fuel and from 143 K to 16 K for coolant. Among the three considered practical factors, the deformed power density from 3-D neutronic outputs affects the thermal-hydraulic performance of TFHR the most. The corresponding temperature rise at fuel compact accounts for 55~65% in total temperature increase. For the effects of helium clearance and graphite properties degradation, the contributions are about 20% and 10 %.

2) With improvements of bypass cooling and mass flow distribution, the temperature distribution throughout the core is flattened with much reduced temperature peaks. Owing to the existence of bypass flow, most heat is transferred within the active core, leading to much lower temperature of outside reflector. It is thus considered a desirable measure for further design of reactor thermal insulation system. Overall, a larger temperature margin, relative to the LSSS limits, has been achieved, even for the case with 20% over-power. It shows feasibility of the current TFHR core design from the thermal-hydraulics prospective.

The other aspects of TFHR research, i.e. tritium control, FLiBe corrosion, materials selection etc., are on-going within the second term of IRP. In this stage, the system design and transient safety analysis of TFHR would be conducted.

ACKNOWLEDGMENTS

Financial support for Chenglong Wang is provided by China Scholarship Council (CSC) and the Chinese National Science Foundation (Grant No. 91326201, No. 11475132). U.S. Department of Energy (DOE) Nuclear Energy University Program (NEUP)-Integrated Research Project of FHR is gratefully acknowledged for funding this work.

REFERENCES

1. C.W. Forsberg, et al., Fluoride-Salt-Cooled High-Temperature Reactors (FHRs) for Base-Load and Peak Electricity, Grid Stabilization, and Process Heat. Department of Nuclear Science and Engineering, Massachusetts Institute of Technology, Cambridge, MA, 2012. **MIT-ANP-TR-147**.
2. K.C. Sun and L.W. Hu. Neutronic Design Features of a Transportable Fluoride-salt-cooled High Temperature Reactor. *Proceedings of ICAPP 2014*. 2014. Charlotte, USA.
3. R. Macdonald and C. W. Forsberg. Strategies for a Small Transportable FHR with Reduced Safety, Security, and Safeguards Systems. *Proceedings of ICAPP 2014*. 2014. Charlotte, USA.
4. C.B. Davis and G.L. Hawkes. Thermal-Hydraulic Analyses Of The LS-VHTR. *ICAPP*. 2006. Reno, NV USA.
5. R.R. Romatoski, L.W. Hu, and C.W. Forsberg. Thermal Hydraulic Licensing Limits for a Prismatic Core Fluoride Salt. *Proceedings of ICAPP 2014*. 2014. Charlotte, USA.
6. M. Richards, et al. Thermal hydraulic optimization of a VHTR block-type core. *Fifteenth International Conference on Nuclear Engineering (ICONE-15)*. 2007. Nagoya, Japan.
7. W.C. Cheng, et al. CFD Analysis for Asymmetric Power Generation in a Prismatic Fuel Block of Fluoride-salt-cooled High-temperature Test Reactor. *Proceedings of ICAPP 2014*. 2014. Charlotte, USA.
8. N.I. Tak, M.-H. Kim, and W.J. Lee, Numerical investigation of a heat transfer within the prismatic fuel assembly of a very high temperature reactor. *Annals of Nuclear Energy*, 2008. **35**(10): p. 1892-1899.
9. B.W. Travis and M.S. El-Genk, Thermal–hydraulics analyses for 1/6 prismatic VHTR core and fuel element with and without bypass flow. *Energy Conversion and Management*, 2013. **67**: p. 325-341.
10. C.W. Forsberg et al., Fluoride-Salt-Cooled HighTemperature Reactors (FHRs) for Base-Load and Peak Electricity, Grid Stabilization, and Process Heat. 2012, Department of Nuclear Science and Engineering, Massachusetts Institute of Technology, Cambridge, MA.
11. M.S. Sohal et al., Engineering Database of Liquid Salt Thermophysical and Thermochemical Properties, Engineering Database of Liquid Salt Thermophysical and Thermochemical Properties. 2010, Idaho National Laboratory.
12. NRC, Guidelines for Preparing and Reviewing Applications for the Licensing of Non-Power Reactors. 1996, Office of NuclearReactor Regulations, Nuclear Regulatory Commission.
13. C.L Wang et al. Thermal-hydraulic Design Features of Transportable Fluoride-salt-cooled High-temperature Reactor. *ANS Annual Meeting*. 2015. San Antonio (Submitted).
14. T. Maruyama and M. Harayama, Neutron irradiation effect on the thermal conductivity and dimensional change of graphite materials. *Journal of Nuclear Materials*, 1992. **195**: p. 44-50.